Geographia Polonica
2016, Volume 89, Issue 1, pp. 91-111
http://dx.doi.org/10.7163/GPol.0048

INSTITUTE OF GEOGRAPHY AND SPATIAL ORGANIZATION
POLISH ACADEMY OF SCIENCES
www.igipz.pan.pl

www.geographiapolonica.pl

APPLICATION OF TIMBERLINE MORPHOMETRIC ANALYSIS FOR DETECTING SNOW AVALANCHE PATHS: A CASE STUDY OF THE TATRA MOUNTAINS

Barbara Spyt[1] • Ryszard J. Kaczka[1] • Michał Lempa[1] • Zofia Rączkowska[2]

[1] Faculty of Earth Sciences
University of Silesia in Katowice
Będzińska 60, 41-200 Sosnowiec: Poland
e-mails: barbaraspyt@wp.pl • ryszard.kaczka@us.edu.pl • 92michal.lempa@gmail.com

[2] Institute of Geography and Spatial Organization
Polish Academy of Sciences
Św. Jana 22, 31-018 Kraków: Poland
e-mail: raczk@zg.pan.krakow.pl

Abstract

The upper forest limit is principally controlled by climate factors, mainly temperature but locally also other factors, such as snow avalanches, debris flows, and wind throw. Therefore, the timberline course may be use as a proxy of these drivers. The aim of the study was to employ the morphometric features of the upper forest limit for remote detection of avalanche paths. We introduced the Morphometric Avalanche Index (*MAI*), which combine simple parameters such as: Perimeter Development, Altitudinal Difference, Elongation Ratio, Area, and the existence forest patches. This tool was tested in four valleys in the Tatra Mountains, wherein 103 known avalanche paths. The employment of *MAI* resulted in remote identification of 90% of avalanche paths existing and acknowledged in this region. Additionally 28 avalanche paths that had not been previously indicated as such were detected.

Key words

snow avalanche • timberline • morphometry • remote sensing • Tatra Mountains

Introduction

The boundary between the forest and the open space above it is recognised as one of the most important natural boundaries (Troll 1972, 1988; Holtmeier 2009; Körner 2012). The division between dense wood vegetation and non-forest area is related to several borderlines: biological (Körner 2003, 2004), climatological (Hess 1965; Walter & Medina 1969; Holtmeier 1974, 2005), and geoecological (Kotarba & Starkel 1972; Troll

1972; Kotarba 1992). At a given location, it results from past and recent interactions among different natural factors (climate, relief, soil) (Wright & Mooney 1965; Bosheng 1993) natural processes (snow avalanches, debris flows, wind, fires, insect outbreaks) (Walsh et al. 1994, 2003), and human interventions (Adamczyk et al. 1980; Price 1981; Sarmiento 2002; Kozak 2005). Although the character and intensity of these drivers vary, in most cases it is possible to identify the predominant one shaping the line at a particular location (Zientarski 1985; Jodłowski 2007). Therefore, the borderline could be recognised not only as a product of different drivers (Allen & Walsh 1996; Holtmeier 2005) but also as a proxy providing information about the character and intensity of the dominant ones (Veblen et al. 1994; Kulakowski et al. 2006). This task requires the utilization of a detailed representation of the forest limit. Among several, broad or specified definitions of the borderline between a dense forest and a non-forest area, the terms timberline (Imhof 1900; Marek 1910; Körner 2012) or empirical timberline (Fries 1913; Sokołowski 1928; Holtmeier 2009) and tree line seem the best such proxies.

The study of timberline features is usually limited to the investigation of the dynamics of the tree dimensions (Paulsen et al. 2000; Kullman 2010) and the species composition of the forest (Walter 1968; Armand 1992). The timberline zone is widely explored by dendrochronologists as a location where the strongest climatic signal may be derived from tree rings (Büntgen et al. 2007, 2008; Lara et al. 2005; Kaczka et al. 2015). Studies of the geometry of the line constituting the forest limit are rare (Treml & Banaš 2000; Treml 2007; Guzik 2008; Shandra et al. 2013) and usually focused on a small area (Czajka et al. 2012; Kaczka et al. 2015; Chhetri 2015). However, recent developments of remote sensing and GIS techniques allow easy access to high quality orthophotomap and create an opportunity to perform complex computations of relatively huge datasets within a short time (Zhao et al. 2014; Czajka et al. 2015b).

Geomorphometric tools are often employed in earth sciences, in research on geomorphological processes and transformations of relief (Pike 2000). Tools of automatic detection are used in the analysis of: i) underwater debris flows (Micallef et al. 2007); ii) landslide flow direction (Niculiță 2015); iii) hydrographic networks and directions of water runoff (Tribe 1992); iv) erosion processes (Buccolini & Coco 2013); and v) an avalanche release zone in the Swiss Alps (Maggioni et al. 2002) and one in the area of Kasprowy Wierch in the Tatra Mountains (Chrustek 2008).

The field observations and the study of recent and historical cartographic materials and scientific reports lead to the statement that snow avalanches are the predominant factor driving the course of the timberline in several mountains of the temperate zone (Ives et al. 1976; Carrara 1979; Butler et al. 1992; Walsh et al. 1994; Veblen et al. 1994), including the Tatra Mountains (Czajka et al. 2012; Kaczka et al. 2015). This process is responsible for local but significant lowering of the timberline course (Fig. 1A and B) and fragmenting of the forest body into separate patches of forest (Fig. 1C). Therefore, the geometry and spatial patterns of the timberline may be linked with the destructive power of the avalanche (Bebi et al. 2009; Kaczka et al. 2015; Czajka et al. 2015c; Lempa et al. 2016). The question whether these features may be quantified and used as a proxy to detect and analyse avalanche paths was the inspiration for the study presented below.

Study area

The study area is located in the Tatra Mountains, the largest and highest massif of the Carpathian arc. The area of the Tatra Mountains covers 785 km^2, and its highest peak is Gerlachovský štít at 2655 m a.s.l. There are more than 3,800 potential avalanche paths there (Žiak & Długosz 2015). The tool detecting avalanche paths influencing the timberline was tested in four major valleys.

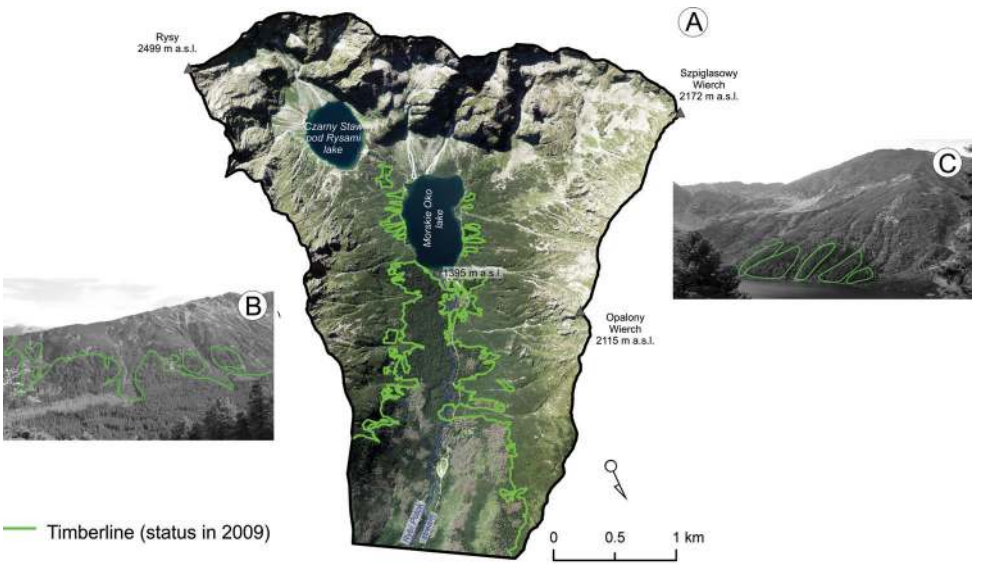

Figure 1. The course of the timberline in the upper part of Rybi Potok Valley (A); view of forest on the slopes of Żabi peak (B) and Szpiglasowy Wierch peak (C). 23% of the timberline is driven by avalanche processes. This leads to the significant lowering of the timberline (B) or creation of patches of forest separated by the avalanche paths (C) (Photos by Ryszard J. Kaczka)

The selected valleys in the Western Tatras were Kościeliska Valley and Žiarska Valley, and in the High Tatras, Mengusovská Valley and Rybi Potok Valley. The studied valleys are situated symmetrically in relation to the main ridge and characterised by northern and southern exposure (Fig. 2). The analyses were focused on the upper parts of the valleys, above 900 m a.s.l., in particular on the zone of the timberline (1030-1640 m a.s.l.). In the study area, there are 103 reported avalanche paths (over 3.5 km^2) exerting a direct impact on the spruce forest (Map 1934; Kłapowa 1976; Map 1999/2000; Žiak & Długosz 2015). Most of them were observed in Kościeliska Valley (55), while the lowest number was observed in Mengusovská Valley (7) (Tab. 1).

Materials and methods

After preliminary analyses of morphological and morphometric characteristics of the known avalanche paths in the area of the Tatras, five morphometric parameters were proposed. Four of them describe the geometrical characteristics of the upper limit of the forest, and one is associated with its altitude above sea level.

The input data was derived from the recent orthophotomaps and Digital Elevation Model. The linear objects were created by mapping limits of the subalpine forest using high resolution satellite orthophotomaps from DigitalGlobe resources (resolution of 0.5 m, accuracy of 10.2 m) taken in 2009 (Mengusovská Valley and Rybi Potok Valley) and 2010 (Žiarska Valley and Kościeliska Valley). Orthophotomaps are made available through the service of World Imagery, ArcMap 10.2 registered by ESRI. The orthophotomaps are available for licensed ArcMap users. Numerical elevation data were obtained from the global, open source of the ASTER GDEM-2 model. ASTER GDEM is a product of METI and NASA. The horizontal resolution of the model is 72 m, and the vertical error for mountain regions is +7.4 m (Tachikawa et al. 2011). Most of the data necessary for following the procedure

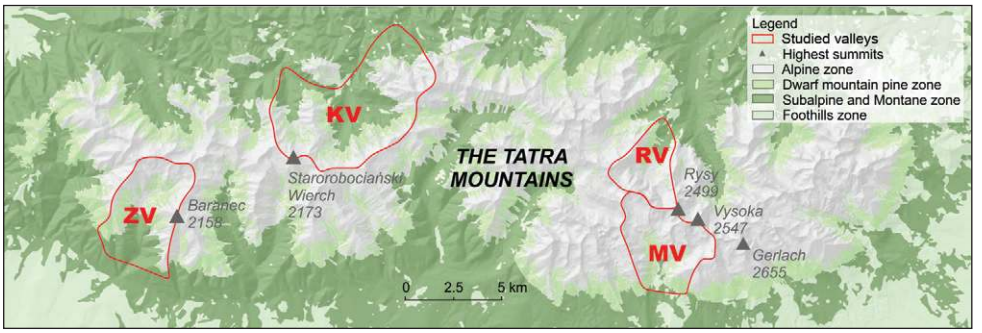

Figure 2. Location of the research area in the Tatra Mountains: KV – Kościeliska Valley; RV – Rybi Potok Valley; MV – Mengusovská Valley; ZV – Žiarska Valley. The shaded relief was produced from GDEM

Table 1. Basic geographical characteristics of the studied valleys

Study area			Kościeliska Valley	Rybi Potok Valley	Mengusovská Valley	Žiarska Valley
Code			KV	RV	MV	ZV
Location			Western Tatras	High Tatras	High Tatras	Western Tatras
Aspect			Northern	Northern	Southern	Southern
Highest peak [m a.s.l.]			Staroroboci Wierch (2,173)	Rysy (2,499)	Vysoka (2,547)	Baranec (2,185)
Minimum altitude [m a.s.l.]			1,035	1,305	1,405	970
Valley area [km^2]			35.2	9.7	15.6	18.4
Land cover	Subalpine forest	km^2	15.1	1.5	1.0	5.4
		%	43	15	6	29
	Dwarf mountain pine zone	km^2	5.5	1.2	2.8	4.1
		%	16	12	18	22
	Alpine zone	km^2	14.6	7.0	11.9	8.9
		%	41	72	76	48
Avalanche paths*	Number		55	21	7	20
	Area [km^2]		1.61	0.53	0.24	1.14

* The total area of avalanche paths reaching the upper limit of the forest – according to reference materials (Map 1934; Kłapowa 1976; Map 1999/2000; Žiak & Długosz 2015).

of semi-automatic detection of avalanche paths are accessible from freely available sources.

Spatial analyses were performed using the ArcMap 10.2 program by Environmental Systems Research Institute (ESRI). Similar analyses may be easily made using other GIS software, which may, however, require minor modifications of the technical aspects of the algorithm employed for the presented analyses.

The first step was to obtain the geometry of the upper limit of the forest data. Photo interpretation of the orthorectified satellite images constituted the basis for determining a detailed course of the timberline (TML) and a more general course of the tree line (TL), both as linear objects. For the purpose of the analyses, timberline was defined as the actual extent of a dense forest with a tree height of at least 8 m and a density above 40% (Fries 1913; Sokołowski 1928; Rubner 1953; Plesnik

1959; Guzik 2008; Czajka et. al 2015a), whereas tree line was defined as the line connecting the uppermost dense forest, which often represents only a potential borderline (Sokołowski 1928; Ellenberg 1958, 1959; Guzik 2008; Holtmeier 2009). The tree line as a whole is a hypothetical line and expresses the maximum extent of the climatic range of the forest (in the case of the Tatra Mountains – thermal) not modified by other natural (avalanches, debris flows, wind fallen trees, etc.) or anthropogenic (pastoralism, tourism infrastructure, forestry clearance) factors (Sokołowski 1928; Holtmeier 2009; Körner 2012) (Fig. 3A).

The linear objects representing the tree line and the timberline obtained through photo interpretation were combined into one linear layer (Fig. 3B). The non-forest areas between the potential line of the maximum extent of the forest (tree line) and its actual position (timberline) were defined and converted into polygon objects (Fig. 3C). These polygons indicate the loss of the forest being the result of operating non-climatic factors and stationary barriers e.g. rocky ridges (Holtmeier et al. 2003; Van Bogaert et al. 2011). The altitudinal and geometric characteristics were assigned to the obtained polygons. Each of the polygons was given an altitude coordinate a.s.l. (Z) acquired from GDEM-2 data by using the *Interpolate shape* tool (Fig. 3C). This procedure consisted of transforming two-dimensional polygons into three-dimensional terrain models (3D polygons). This measure was used to identify non-forest areas as elements of the environment closely correlated with the terrain. Furthermore, basic parameters, such as the area (A) and perimeter (P) were assigned to the polygons.

For each of the generated polygons, Altitudinal Difference above sea level was calculated using the formula (Fig. 4A):

$$AD = Max_{altitude} - Min_{altitude}$$

This indicator, along with the Elongation Ratio, helps differentiate the polygons located parallel to the slope inclination from the polygons oriented perpendicular to the slope inclination. Both of these features facilitate determining the position of non-forest polygons in relation to the slope.

The next step was to determine the shape of the individual non-forest areas, which was done using indexes describing the ratio of the polygon elongation and the complexity of the polygon shape (Figs. 4B and 4C).

The Elongation Ratio indicates how much the shape of the polygon is different from the shape of the circle. It is a measure adopted from hydrology, wherein it defines the ratio of the elongation of the catchment (Basin Elongation Ratio) (Schumm 1956). This parameter is calculated through the following formula:

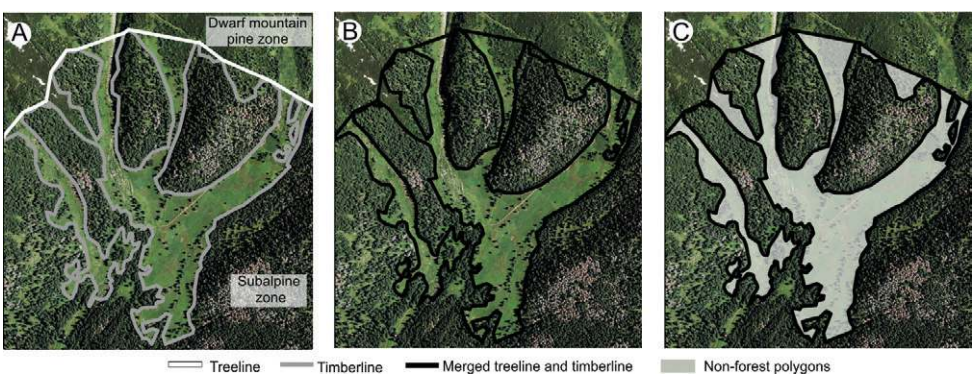

Figure 3. The spatial difference between the course of the tree line and the timberline (A). An example of merging of linear objects (B) into the polygons representing the non-forest area resulted from the reduction of the forest extent (C)

$$ER = \frac{2}{L_{max}\sqrt{\frac{A}{\pi}}}$$

ER – polygon Elongation Ratio
A – polygon area
L_{max} – maximum polygon diameter

The parameter values are in the range of 0 to 1, where 1 is a circle-shaped polygon (Fig. 4B). The indicator of Elongation Ratio was calculated using the tool of *polygon thickness* in the package of EasyCalculate10, which is an add-in control to ArcMap 10 ESRI (Tchoukanski 2012). The *A* and L_{max} parameters are calculated through that tool.

The indicator of Perimeter Development (*PD*) (Fig. 4C) is a modified measure also coming from hydrology (indicator of shoreline development) (Hutchinson 1957; Hakanson 1981). It allows determining the degree of the complexity of the perimeter, here the shape of the polygon.

$$PD = \frac{P}{2\sqrt{\pi A}}$$

PD – Perimeter Development
P – perimeter of the polygon
A – area of 2D polygon

On the basis of the field observations and map analyses the frequent association of separated forest patches within avalanche paths was identified (from 7 in Mengusovská Valley to 29 in the Rybi Potok Valley) (Fig. 1C). This takes place when two or more avalanche paths merge into a larger one. The merging of the tree line and timberline line objects results in creating a spatial pattern of the forest polygons accompanied by non-forest polygons. The forest polygons occurring in such patterns were so-called Inner Forest polygons (IF) (Fig. 4D). The complexity of the configuration of forest and non-forest polygons increases with the number of merging avalanche paths. In order to semi-automatically determine the occurrence of inner forest polygons, two tools of EasyCalculate10 were employed: *shape_CountAllParts* and *polygon_CountTrueParts*. The first one calculates the number of the polygon segments, while the second one counts fragments of the polygons to the exclusion of cavities (non-forest polygons). The result of the logical function of the difference between these two indicators points out the occurrence of inner forest polygons ($IF > 1$) or the lack of them ($IF = 0$).

Besides the four morphometric parameters described above, the area of the non-forest polygon was selected as an additional indicator. The polygons of a larger surface area are more likely to be of avalanche origin. The smallest of them (the total of 10% in all 4 valleys), characterised by an area $< 15 m^2$, are most likely artefacts resulting from the merger of two empirically drawn lines: timberline and tree line. These types of polygons are excluded using weighted index.

Compilation of all the parameters (Area, Perimeter Development, Elongation Ratio, Altitudinal Difference and Inner Forest) allows determining the probability of the avalanche influence on the difference, which arose between TL and TML. For the model calibration 50 locations where the timberline is distinctly lower in comparison to the tree line was chosen. 25 of these locations are confirmed avalanche paths, and the remaining 25 are locations where no avalanche activity was ever recorded. The selection was random and the only criterion was in relation with avalanches. The variability of each parameter was analysed in both groups and the threshold values for each parameter was assessed (Fig. 5). Statement of all thresholds for all parameters allowed for initial interpretation of the origin of non-forest polygons and their division into four groups: avalanche, likely avalanche, unlikely avalanche and no-avalanche polygon. The parameterisation process and model calibration were done using a trial and error method, while the results were subject to expert validation (Stacey & MacGregor 1999).

The next step was to increase the unification of the results by eliminating two intermediate groups and leaving only two definitive

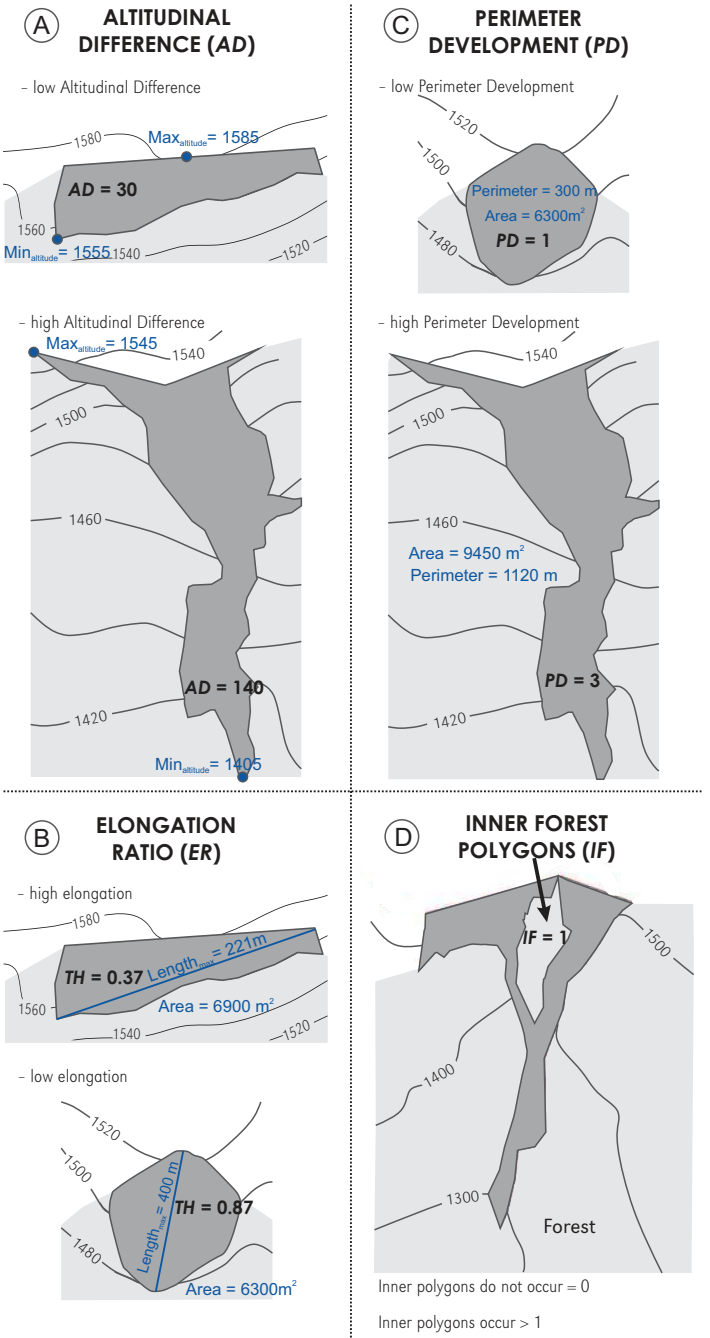

Figure 4. Examples of four morphometric parameters used for describing non-forest polygons: A – Altitudinal Difference (AD); B – Elongation Ratio (TH); C – Perimeter Development (PD); D – Inner Forest Polygons (IF)

options: avalanche polygons and no-avalanche polygons. The weighting procedure was performed. The threshold values are given four weights: two weights informing about the avalanche origin of the polygon (weight 2 and 1) and two describing other polygons (weight –1 and –2) (Fig. 6). It was decided not to use neutral weight 0 to clearly separate the polygons of varying origin. The sum of the weights of the five parameters enabled calculating the Morphometric Avalanche Index (*MAI*).

The values of *MAI* for the 389 analysed polygons are in the range from –4 to 9. Empirical tests were carried out for all the polygons to establish the reliable threshold value of *MAI* (Fig. 6), which distinguishes non-forest areas resulting from avalanche processes ($MAI \geq 4$) (and subsequently called the avalanche polygon) from those related to other factors ($MAI < 4$) (no-avalanche polygon).

Because generating non-forest polygons is sensitive to tree line/timberline position, not to the existence of actual, individual avalanche paths, the final stage involved dividing, if necessary, polygons into the individual avalanche paths. This step is vital because the whole process often produces polygons with more than one avalanche path. In the study area, 24% of all the avalanche polygons represent two or more neighbouring avalanche paths (Fig. 7). The process of identifying whether the polygon is associated with one or several paths and sorting out the individual paths was based on:

- the shape of the polygon,
- existence of IF, and
- the analyses of relief (Numerical elevation data were obtained from the global, open source of ASTER GDEM-2 model).

As reference data the cartographic documentations of known avalanche paths were employed:

- a winter ski map of the Polish Tatras from 1934, at a scale of 1: 20,000 (Map 1934);
- maps from "Avalanche danger in the Polish Tatras" by Kłapowa (1976) resulting from field mapping in the winter of 1969/1970;
- the tourist map of "the Polish Tatras – winter version", at a scale of 1: 25,000, with avalanche paths marked on the day of 28 January 2003 (Map 1999/2000);
- maps of potential avalanche paths for the entire Tatras (Žiak 2012; Žiak & Długosz 2015).

The verification procedure consisted of confronting the polygons indicated by the *MAI* with ones indicated on the maps. The results of the verification fell into five categories (Fig. 8):

- polygons detected by the algorithm as non-avalanche ones ($MAI < 4$) and confirmed as such by the cartographic data,

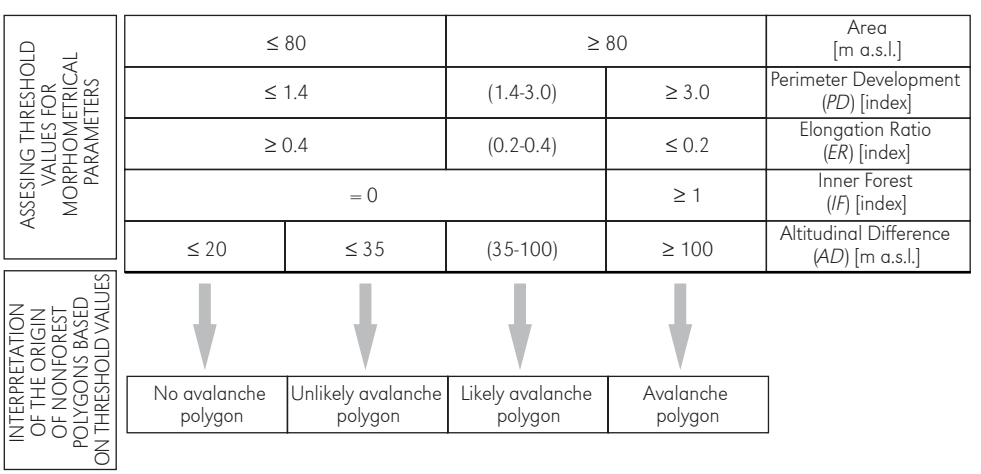

Figure 5. Scheme describing the procedure of the non-forest polygons features parametrisation

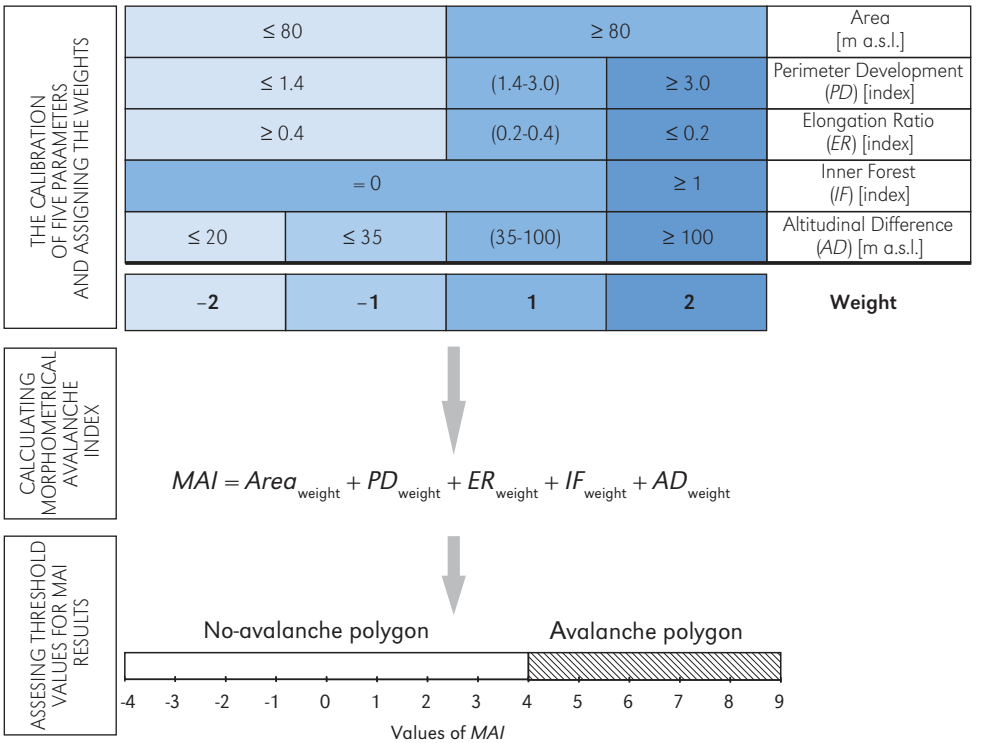

Figure 6. Scheme describing the procedure of the extraction the avalanche polygons based on employment of five parameters and Morphometric Avalanche Index

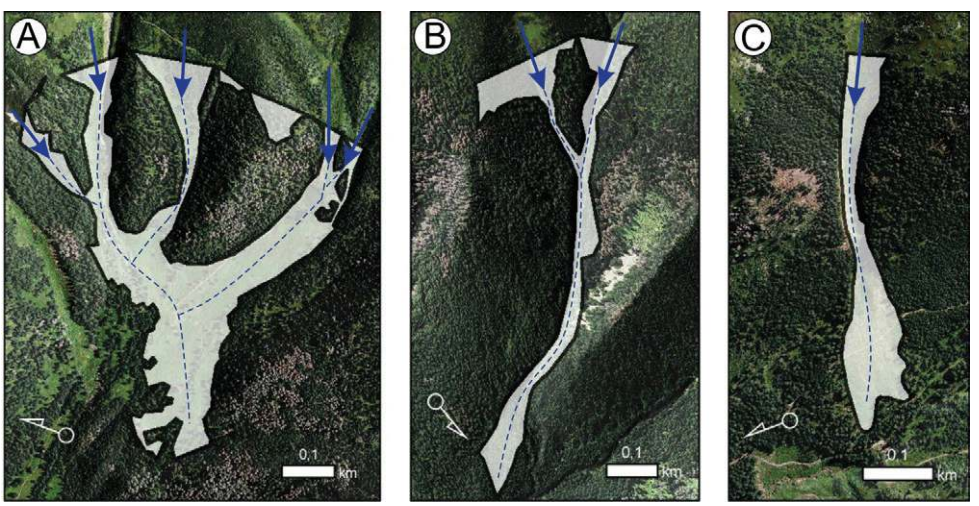

Figure 7. Avalanche polygon and avalanche path: complex avalanche polygon compounded of five avalanche paths (A); avalanche polygon composited from two avalanche paths (B); typical, singular, elongated avalanche polygon (C)

- polygons detected by the algorithm as non-avalanche ones (*MAI* < 4) and indicated by other sources as real avalanche paths. Therefore these so-called *undetected avalanche polygons* were recognised as an error,
- polygons detected by the algorithm as avalanche ones (*MAI* ≥ 4) and indicated as such on the maps,
- polygons detected by the algorithm as avalanche ones (*MAI* ≥ 4), not indicated on the maps, however exhibiting other features of avalanche paths. These are potential locations wherein avalanche hazard exists but has not yet been indicated on the maps,
- polygons detected by the algorithm as avalanche ones, although not confirmed by cartographic, relief and other sources. Therefore, these so-called *false avalanche polygons* were recognised as an error.

Results and discussion

Within the four studied valleys, totals of 185 km of timberline and 43 km of tree line were determined. The proportion of the length of these lines (TL represents only 23% of TML) indicates how strongly non-climatic factors shape the upper limit of the forest in the study area. This influence is the most significant in Žiarska Valley and Kościeliska Valley and the weakest in Mengusovská Valley (respectively 24%, 25% and 41%). These observations coincide with the number of avalanche paths per valley (Fig. 9). The differences are the result of many variables, e.g. the area of study, the shape of the valley, the exposure of the valley and the altitudinal difference between the lowest and the highest point. The described changes in the timberline may also be caused by other processes such as debris flows and rockfalls. However, in the whole Tatra Mountains, including the studied valleys, merely a few of them bring about alteration of the boundary of the subalpine forest (Jurczak et al. 2012; Długosz 2015). Therefore, in the examined cases mass movements can be excluded as such factors, and it can be presumed that in the study area avalanches are the most important non-climatic factor modifying the course of the upper limit of the subalpine forest. In his detailed studies Guzik (2008) demonstrated that timberline changes in the Polish Tatras were intensive but locally. It is mainly up-shift of the timberline and tree line and increase of forest area without any significant vertical

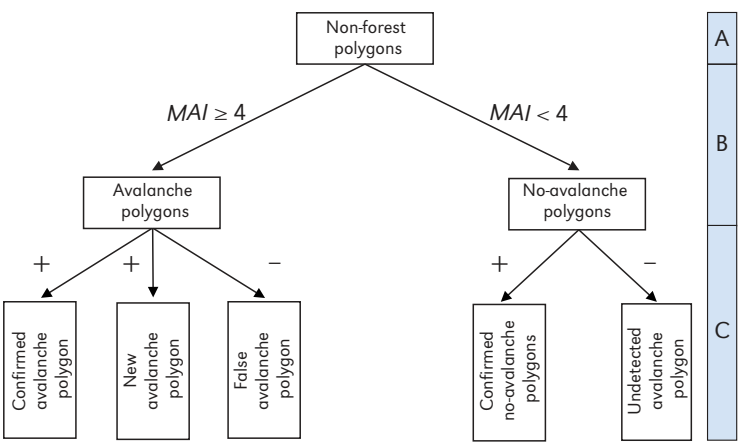

Figure 8. The verification of *MAI* results in comparison with historical records and cartographic data. The non-forest polygons generated as a space between tree line and timberline (A), divided into two groups (avalanche and non-avalanche polygons) based on the *MAI* index results (B). The validation of the results by comparisons of *MAI* classification of 50 polygons with the existing information about the avalanche paths ("+" indicates the correct, and "-" incorrect results of *MAI* implementation)

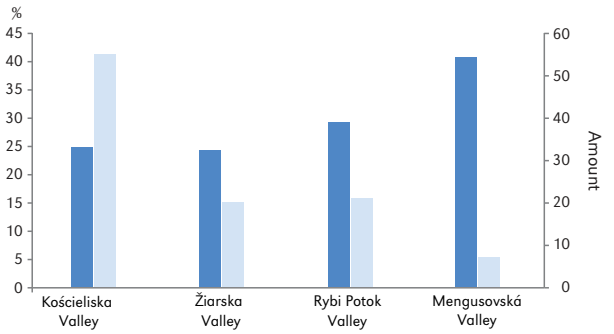

Figure 9. The ratio of the length of TL to the length of TML (dark blue) in comparison to the amount of the existing avalanche paths (light blue) (according to all the reference maps) in the four studied valleys

direction. Those changes are mainly connected with modification of land use; nevertheless, pronounced warming is observed in the studied region (Żmudzka 2011).

In the study area, the non-forest area between the tree line and the timberline consists of 389 individual polygons of a total area of 4.3 km^2 (Fig. 10). The highest number of the non-forest polygons was identified in Kościeliska Valley (176), and the smallest in Rybi Potok Valley (52) (Fig. 11).

The surface areas of particular polygons exhibit substantial differences in size (Fig. 12A), from very small (less than 100 m^2) to the polygons of an area of 0.8 km^2 (Žiarska Valley). Most of them, however, have a surface area within the range of 147-3775 m^2. In all of the valleys, non-forest polygons containing inside patches of forest (inner forest polygons) were also observed. That type of avalanche path appears in all study areas. Inner forest polygons are presented on convex forms localized between parallel paths. The indicator of Perimeter Development, describing the complexity of the shape, ranged from 1.4 to 2.2 for the majority of the polygons (54%) (Fig. 12B). The PD values outside this range were used to determine the nature of the polygon. High values of PD (> 3; 14% of the cases) were obtained for the polygons of the avalanche origin but also for those resulting from human activities (e.g. Fig. 11a). Anthropogenic polygons are in many cases characterized by elongated and complex shapes. Such shapes are an effect of clearings on ridges or high altitude glades or of active pasturing in the forest (the last has not occurred recently in the Tatras). They could be differentiated from avalanche polygons by the Altitude Difference parameter. The polygons characterised by low PD values (< 1.4; 21% of their amount) do not meet the criterion of the shape empirically identified as associated with avalanches.

On the basis of the value of the altitudinal difference calculated for non-forest polygons, 65% of them were excluded as those, which had not resulted from the avalanche activity. The small area (< 35 m) is common feature of this group of polygons (Fig. 12C).

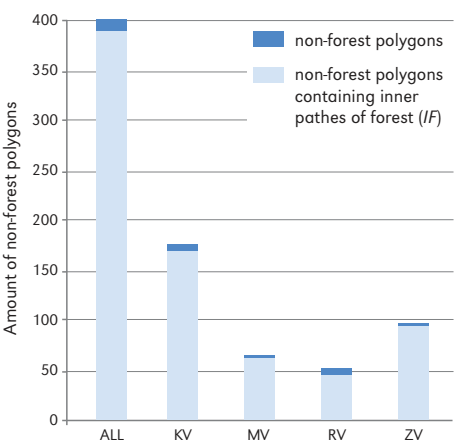

Figure 10. The number of non-forest polygons and polygons with inner forest in the studied valleys (KV – Kościeliska Valley; MV – Mengusovská Valley; ZV – Žiarska Valley; RV – Rybi Potok Valley)

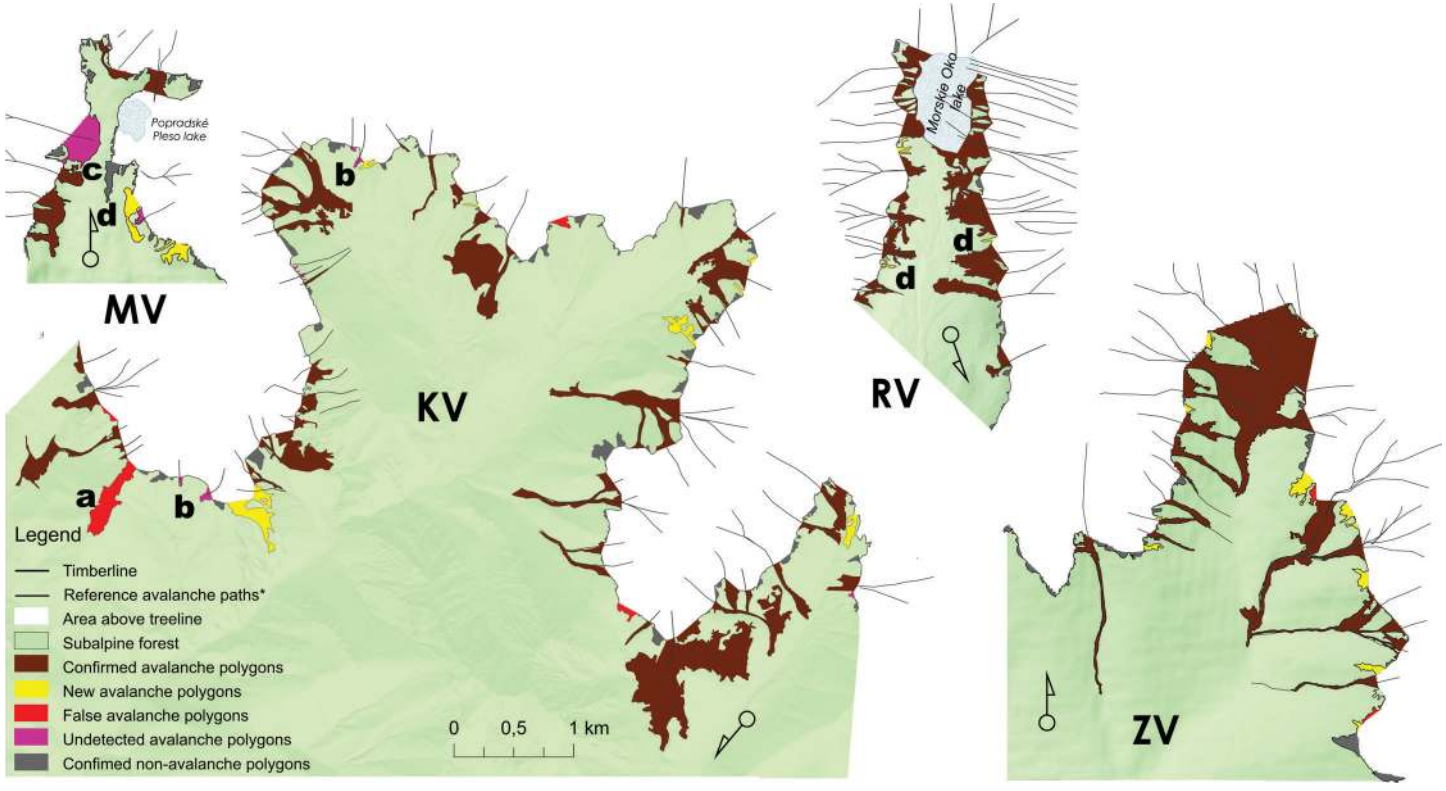

Figure 11. Spatial distribution of the five types of avalanche polygons in the studied valleys: Kościeliska (KV), Mengusovká (MV), Žiarska (ZV) and Rybi Potok (RV). Grey lines indicate avalanche path marked at reference maps. Examples of the polygons of: a) false avalanche paths (anthropogenic polygon); b) small undetected avalanche paths; c) shallow, fan-shaped undetected avalanche paths; d) avalanche paths detected exclusively by the algorithm

The identification of the polygons associated with avalanches was greatly facilitated by use of the extreme values of the indicator of Elongation Ratio (Fig. 12D). The polygons of ER values > 0.4 (a shape similar to a circle) represent 40% of all the polygons. The polygons exhibiting such a shape are excluded from the group associated with avalanches. In contrast, 25% of the polygons are characterised by ER value < 0.2 indicating an elongated shape, which, with a high degree of probability, was the result of the activity of avalanches.

Based on the results of the calculations of the weight index of *MAI* constituting the compilation of the 5 parameters, 97 non-forest polygons (25% of all the polygons) were identified as avalanche associated. They occupy a total surface of 3.92 km^2 (91% of all the non-forest polygons) (Tab. 2). Verification of the algorithm showed that it correctly identified 52 avalanche polygons (Tab. 2), which represent 90% of all the avalanche paths indicated in all the reference materials, and stand for 97% of the area of all the avalanche

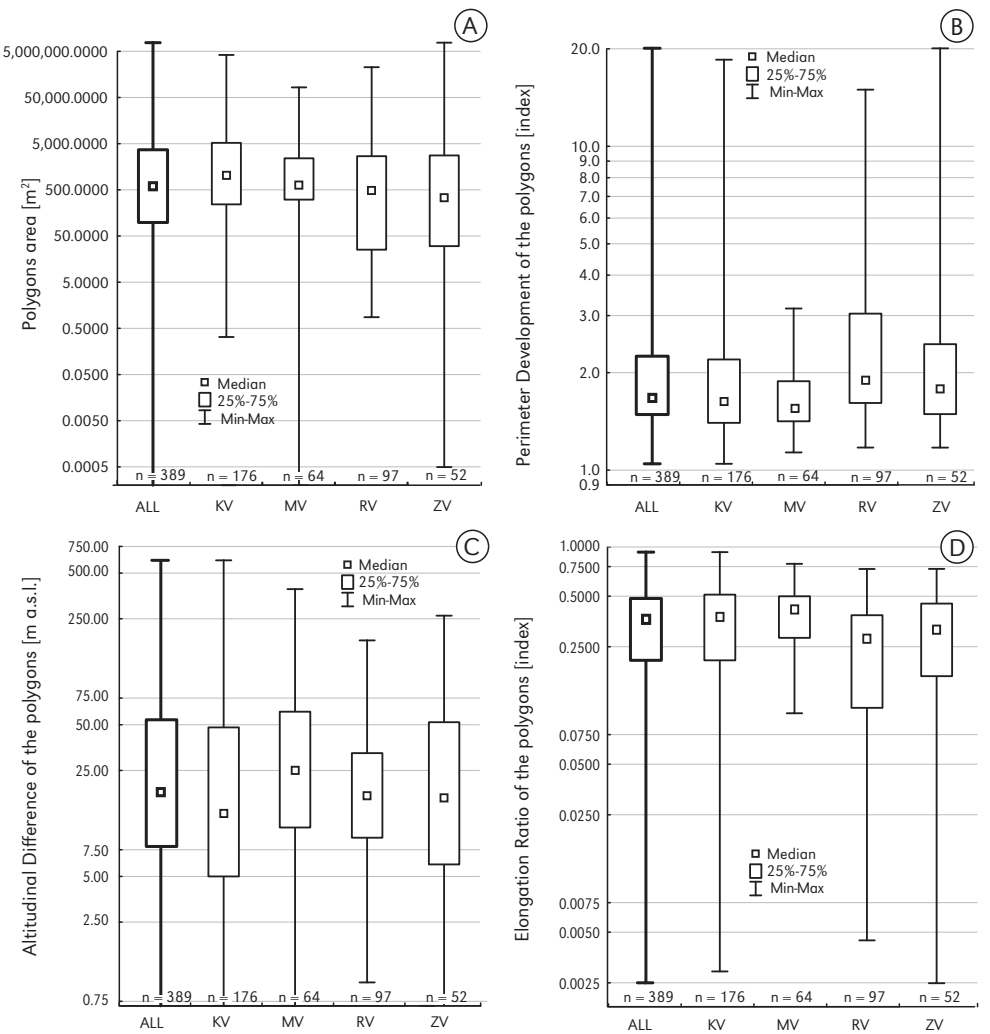

Figure 12. Morphometric features of the non-forest polygons: area (A), Perimeter Development – PD (B), Altitudinal Difference – AD (C) and Elongation Ratio – ER (D)

paths. In two valleys (Rybi Potok Valley and Žiarska Valley), the algorithm exhibited 100% accuracy.

Among the other polygons are those whose relationship with avalanches is impossible or questionable. The first ones comprise deforestation resulting from logging, wind throw or represent a low position of the timberline associated with orographic barriers. The second ones are composed of a heterogeneous group of the areas whose morphometric characteristics did not allow for clear classification.

In 10% of the studied polygons, *MAI* results did not point out the avalanche origin of the polygons, which actually are avalanche paths. Such undetected avalanche polygons represent 3% of the area of all the analysed polygons. These polygons are characterised by a small size (an area less than 0.008 km^2), rounded (*ER* < 0.31) and poorly developed shape (*PD* < 1.8) as well as a small difference in altitude (*AD* < 75 m) (Fig. 13A-D). Their *MAI* scores ranged from –2 to 3 (Fig. 14), well below the adopted threshold. Such cases of avalanche polygons are rare on the scale of the Tatra Mountains, which entails difficulties in the empirical calibration of the range of *MAI* values ensuring their detection. This applies mainly to the avalanches whose run-out zone only slightly overlaps the timberline, thus lowering the timberline by not more

Table 2. The results of employing the Morphometric Avalanche Index (*MAI*) for detecting avalanche paths in individual valleys.

	All avalanche detections	Valid avalanche detection		Errors	
		confirmed avalanche polygons	new avalanche polygons	false avalanche polygons	undetected avalanche polygons
Kościeliska Valley					
Avalanche polygons	53	32	8	5	8
Avalanche paths	68	47	8	5	8
Area [km^2]	1.82	1.59	0.11	0.10	0.02
% of the avalanche polygons area	100.0	87.7	6.1	5.3	0.9
Rybi Potok Valley					
Avalanche polygons	14	9	5	-	-
Avalanche paths	27	21	6	-	-
Area [km^2]	0.58	0.53	0.05	-	-
% of the avalanche polygons area	100.0	91.0	9.0	-	-
Mengusovská Valley					
Avalanche polygons	10	4	4	-	2
Avalanche paths	11	5	4	-	2
Area [km^2]	0.30	0.15	0.06	-	0.09
% of the avalanche polygons area	100.0	51.0	19.4	-	29.6
Žiarska Valley					
Avalanche polygons	20	7	10	3	-
Avalanche paths	33	20	10	3	-
Area [km^2]	1.23	1.14	0.08	0.01	-
% of the avalanche polygons area	100.0	93.0	9.2	0.8	-
Sum					
Avalanche polygons	97	52	27	8	10
Avalanche paths	139	93	28	8	10
Area [km^2]	3.92	3.45	0.26	0.11	0.10
% of the avalanche polygons area	100.0	88.1	6.5	2.7	2.7

than 35 m (Fig. 11b). Among undetected avalanche polygons, there is only one of a large surface area (0.08 km^2). The morphometric parameters of this polygon also differ from the typical characteristics of the local avalanche polygon. It is an uncommon type of the avalanche path of a little inclination and a shallow, fan-shaped area of the runout zone (Fig. 11c). This unique type of avalanche path was observed only in Mengusovská Valley. The highest number of undetected avalanche polygons was recorded (8 of 10) in Kościeliska Valley, although it represents less than 13% in this valley and 1% of all the studied avalanche polygons (Tab. 2). In Mengusovská Valley, wherein the lowest number of avalanche paths is present, the algorithm indicated 2 undetected avalanche polygons. In Žiarska Valley and Rybi Potok Valley, errors of this type did not occur.

The second type of error, false avalanche polygons, constituted 10% of the analysed cases (0.11 km^2 representing 2.7% of the area of the studied polygons). False avalanche polygons are generated when average values of 4 parameters and a high value of one is obtained (Fig. 11A-D): a large altitudinal difference (*AD* > 100 m^2; 2 polygons), a strongly elongated shape (*ER* < 0.2; 2 polygons), or a significant development of the perimeter (*PD* = 3.3; 1 polygon). For this reason, their values of *MAI* are not very high, although

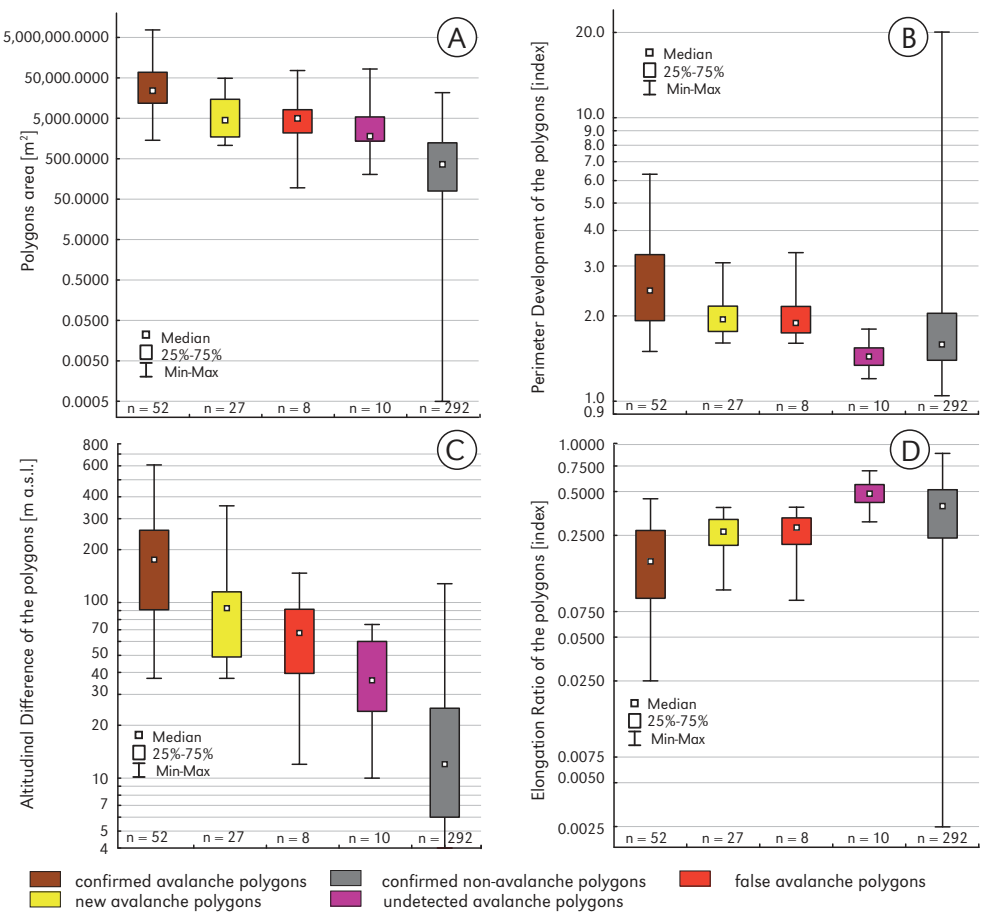

Figure 13. Morphometric characteristics of five categories of non-forest polygons: Area (A), Perimeter Development – PD (B), Altitudinal Difference – AD (C) and Elongation Ratio – ER (D)

still above the threshold ranging from 4 to 6 (Fig. 14). None of the misclassified polygons comprised inner forest patches, which seems to be an essential feature of the polygons of avalanche origin. Errors of this type were observed only in Kościeliska Valley (5 polygons) and Žiarska Valley (3 polygons).

28 polygons (21% of all the avalanche polygons, *Area* = 0.26 km^2) were detected as avalanche polygons, which had not been indicated on any reference maps (Tab. 2). These polygons are characterised by values of *MAI* from 5 up to the highest 9 (Fig. 14). In each valley, from 4 (Mengusowská Valley) to 10 (Žiarska Valley) previously unidentified avalanche paths are present (Tab. 2). Half of them are typical in terms of morphometry: extended avalanche paths of a steep inclination and a varied shape (Fig. 13A-D, Fig. 11d). The remaining group of the new avalanche polygons is related to the dyna-mics of the process of avalanches. Based on the analysis of the limit of the forest, it was determined that the recent course and extent of avalanches (2009-2010) is different from those existing on earlier maps (1934, 1976) (Czajka et al. 2012; Kaczka et al. 2015). The obtained results might be also related to the inaccurate

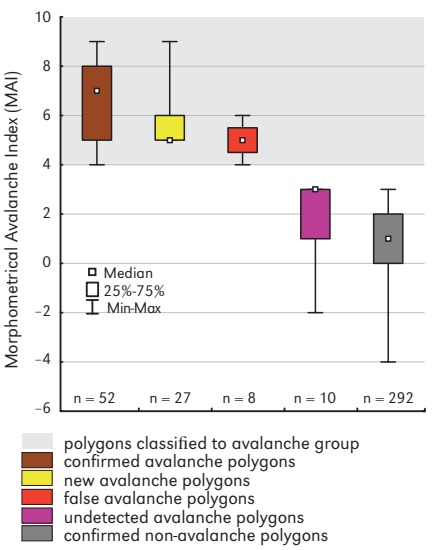

Figure 14. Basic statistics of five classes of non-forest polygons derived from value of *MAI*

indications of avalanche paths on the existing maps (Czajka et al. 2010). The field observations, analyses of the historical timberline location, and analyses of the relief within the avalanche polygon and above it pointed to the conclusion that these polygons are of actual avalanche origin.

The final stage of analyses was deriving information about the actual avalanche paths from polygon analyses. 131 avalanche paths exerting direct impact on the forest of the surface of 3.81 km^2 were detected. They constitute approximately 42% of all the avalanche paths in the study area. In terms of morphometry, the majority of the avalanche paths are vast elongated areas of orientation perpendicular to the slope, varied shapes and significant inclination. Within their range, there are frequent patches of forest separated from the subalpine forest by gullies. The spatial correlation of the non-forest polygons with the reference to avalanche paths proved that 57 confirmed avalanche polygons represent 93 avalanche paths (Fig. 15). Some of the detected avalanche paths, in the lower part of their course, merge to form one major avalanche path (Fig. 3). *MAI* index identified 90% of the avalanche paths being marked on the cartographic reference materials. It also correctly detected all the avalanche paths typical in terms of morphometry. A major achievement of this method is identification of new avalanche paths, unmarked in the previous cartographic materials, which constitute 21% of all avalanche paths in the four studied valleys. The real avalanche character of the indicated paths has to be positively verified by independent sources, e.g. field observations.

Challenges and possible solutions

The greatest challenge of the established method is detecting large, convex and shallow avalanche paths in the shape of a fan, and small avalanche paths, which only slightly modify the TML forest. One possible solution is to include additional morphometric parameters, e.g. the shape of the slope (concave

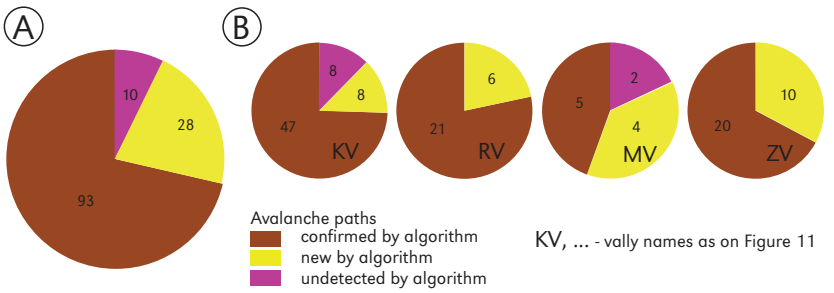

Figure 15. The avalanche paths in agreement with the database, those detected only by algorithm, and miscalculated *MAI*. (A) - the Tatra Mountains; (B) - analysed valleys seperatly. The use of *MAI* in two of the four valleys detected all previously indicated avalanche paths and exceeded the existing knowledge

or convex) located within the polygon and above it. This would exclude errors arising from classifying small areas within a small ridge into the avalanche group, and could simultaneously allow detection of extensive and convex accumulation cones in the bottoms of the valleys, above which troughs of a concave shape of the slope are present.

It should be also noted that the robustness of the proposed method depends on the accuracy of input data, especially linear objects representing the timberline and the tree line, determined through photo interpretation. In turn, their accuracy depends on the resolution of satellite or aerial images as well as the on the preciseness and expertise of the person performing their orthorectification and photointerpretation (Kaczka et al. 2015).

Improvement of the method could also include developing a tool for semi-automatically dividing the positively verified and new avalanche polygons into avalanche paths.

The implementation of the *MAI* algorithm in regions other than the Tatra Mountains might also require the calibration of threshold in local environments.

Conclusions

- The combined course of the treeline and the timberline are a good indicator of avalanche paths.
- The *MAI* index (Morphometric Avalanche Index) incorporating five morphometric parameters was developed. Applying *MAI* resulted in the detecting of 71% (Mengusovská Valley) to 100% (Rybi Potok Valley and Žiarska Valley) avalanche paths indicated in the existing cartographic materials. In total, for all four tested valleys 90% of the avalanches were indicated.
- It was possible, by using the algorithm, to point out some new locations where avalanches have not been recorded but probably occurred. The new method detected from 12% (Kościeliska Valley) to 36% (Mengusovská Valley) more avalanche paths than are indicated on the existing maps and other sources of information.
- In the studied area, the biggest challenge was to detect big and shallow, fan-shaped avalanche paths and small avalanche paths that only slightly encroach the subalpine forest. This kind of the avalanche path constitutes ~3% of the whole studied population.

Acknowledgments

This study was financed from the funds of the research project of National Science Centre No. 2011/03/B/ST10/06115 "Avalanche activity in the Tatra Mountains as an indicator of environmental changes during the last 200 years."

Editors' note:
Unless otherwise stated, the sources of tables and figures are the authors', on the basis of their own research.

References

Adamczyk B., Gerlach T., Obrębska-Starklowa B., Starkel L., 1980. *Zonal and azonal aspects of the agriculture forest limit in the Polish Carpathians*. Geographia Polonica, vol. 43, pp. 71-84.

Allen T.R., Walsh S.J., 1996. *Spatial and compositional pattern of alpine treeline, Glacier National Park, Montana*. Photogrammetric Engineering and Remote Sensing, vol. 62, no. 11, pp. 1261-1268.

Armand A.D., 1992. *Sharp and gradual mountain timberlines as a result of species interaction*. Ecological Studies, vol. 92, pp. 360-378.

Bebi P., Kulakowski D., Rixen C., 2009. *Snow avalanche disturbances in forest ecosystems – State of research and implications for management*. Forest Ecology and Management, vol. 25, no. 9, pp. 1883-1892.

Bosheng L., 1993. *The alpine timberline of Tibet* [in:] J. Alden, J.L. Mastrantonio, S. Odum (eds.), Forest development in cold climates, New York: Plenum Press, pp. 511-527.

Buccolini M., Coco L., 2013. *MSI (morphometric slope index) for analyzing activation and evolution of calanchi in Italy*. Geomorphology, vol. 191, no. 2, pp. 142-149.

Butler D.R., Malanson G.P., Walsh S.J., 1992. *Snow-avalanche paths: conduits from the periglacial– alpine to the subalpine – depositional zone*. [in:] J.C. Dixon, A.D. Abrahams (eds.), Periglacial Geomorphology. Wiley, London, pp. 185-202.

Büntgen U., Frank D.C., Kaczka R.J., Verstege A., Zwijacz-Kozica T., Esper J., 2007. *Growth/climate response of a multi-species tree-ring network in the Western Carpathian Tatra Mountains, Poland and Slovakia*. Tree Physiology, vol. 27, no. 5, pp. 689-702.

Büntgen U., Frank D.C., Wilson R., Career M., Urbinati C., Esper J., 2008. *Testing for tree-ring divergence in the European Alps*. Global Change Biology, vol. 14, no. 10, pp. 2433-2453.

Carrara P.E., 1979. *The determination of snow avalanche frequency through tree-ring analysis and historical records at Ophir, Colorado*. Geological Society of America Bulletin, vol. 90, pp. 773-780.

Chhetri P.K., 2015. *Use of high resolution DigitalGlobe satellite imagery to map the alpine treeline ecotone of the Nepal Himalaya*. Digital Glob Funadation.

Chrustek P., 2008. *Using GIS to estimate the avalanche release hazard level: The case of Kasprowy Wierch, Tatra Mts*. Annals of Geomatics, vol. 6, no. 1, pp. 41-48.

Czajka B., Kaczka R.J., Guzik M., 2010. *Zapis lawin śnieżnych w przebiegu górnej granicy lasu w Tatrach Zachodnich*. Z badań nad wpływem antropopresji na środowisko, vol. 12, pp. 26-38.

Czajka B., Kaczka R.J., Guzik M., 2012. *Zmiany morfometrii szlaków lawinowych w Dolinie Kościeliskiej od utworzenia Tatrzańskiego Parku Narodowego* [in:] A. Łajczak et al. (eds.), Antropopresja w wybranych strefach morfoklimatycznych – zapis w rzeźbie i osadach. Prace Wydziału Nauk o Ziemi Uniwersytetu Śląskiego, 77, Sosnowiec: Wydział Nauk o Ziemi Uniwersytetu Śląskiego, pp. 126-135.

Czajka B., Łajczak A., Kaczka R.J., Nicia P., 2015a. *Timberline in the Carpathians: An overview*. Geographia Polonica, vol. 88, no. 2, pp. 7-34.

Czajka B., Łajczak A., Kaczka R.J., 2015b. *Geographical characteristics of the timberline in the Carpathians*. Geographia Polonica, vol. 88, no. 2, pp. 35-54.

Czajka B., Łajczak A., Kaczka R.J., 2015c. *The influence of snow avalanches on the timberline in the Babia Góra Massif, Western Carpathians*. Geographia Polonica, vol. 88, no. 2, pp. 147-162.

Długosz M., 2015. *Spływy gruzowe*. Map at a scale of 1:100,000 (sheet V.2) [in:] K. Dąbrowska, M. Guzik (eds.), Atlas Tatr. Przyroda nieożywiona, Zakopane: Tatrzański Park Narodowy.

Ellenberg H., 1958. *Wald oder Steppe? Die natürliche Pflanzendecke Perus*. Umschau, vol. 21, pp. 645-648; Umschau vol. 22, pp. 679-681.

Ellenberg H., 1959. *Typen tropischer Urwälder in Peru*. Schweizerische Zeitschrift für Forstwesen, 110, Zürich: Forstverein, pp. 169-187.

Fries T.C.E., 1913. *Botanische Untersuchungen im nördlichsten Schweden: Ein Beitrag zur Kenntnis der alpinen und subalpinen Vegetation in Torne Lappmark. Vetenskapliga och praktiska undersökningar i Lappland*. Flora ich Fauna, 2, Uppsala: Almqvist & Wiksells.

Guzik M., 2008. *Analiza wpływu czynników naturalnych i antropogenicznych na kształtowanie się zasięgu lasu i kosodrzewiny w Tatrach*. Kraków: Uniwersytet Rolniczy im. Hugona Kołłątaja.

Wydział Leśny. Katedra Botaniki Leśnej i Ochrony Przyrody [PhD thesis].

Hakanson L., 1981. *A manual of lake morphometry*. New York: Springer-Verlag Berlin Heidelberg.

Hess M., 1965. *Piętra klimatyczne w polskich Karpatach Zachodnich*. Zeszyty Naukowe Uniwersytetu Jagiellońskiego. Prace Instytutu Geograficznego, 33, Kraków: Uniwersytet Jagielloński.

Holtmeier F.K., 1974. *Geooekologische Beobachtungen und Studien an der subarktischen und alpinen Waldgrenze in vergleichender Sicht*. Wiesbaden: Franz Steiner.

Holtmeier F.K., 2005. *Relocation of snow and its effects in the treeline ecotone-with special regard to the Rocky Mountains, the Alps and northern Europe*. Erde, vol. 136, no. 4, pp. 343-373.

Holtmeier F.K., 2009. *Mountain timberlines: Ecology, patchiness, and dynamics*. Advances in Global Change Research, 36, New York: Springer Science & Business Media.

Hutchinson G.E., 1957. *A treatise on limnology: Vol. 1. Geography, Physics and Chemistry*. New York: Wiley.

Imhof E., 1900. *Die Waldgrenze in der Schweiz, Gerlands Beitr*. Gerland's Beitrage zur Geophysik, vol. 4, no. 3, Leipzig: Engelmann, pp. 241-330.

Ives J.D., Mears A.I., Carrara P.E., Bovis M.J., 1976. *Natural hazards in mountain Colorado*. Annals of the Association of American Geographers, vol. 66, no. 1, pp. 129-144.

Jodłowski M., 2007. *Górna granica kosodrzewiny w Tatrach, na Babiej Górze i w Karkonoszach: Struktura i dynamika ekotonu*. Kraków: Instytut Geografii i Gospodarki Przestrzennej Uniwersytetu Jagiellońskiego.

Jurczak P., Migoń P., Kaczka R.J., 2012. *Występowanie i wybrane cechy morfometryczne szlaków spływów gruzowych w Tatrach i Karkonoszach*. Czasopismo Geograficzne, vol. 83, no. 1-2, pp. 29-46.

Kaczka R.J., Lempa M., Czajka B., Rączkowska Z., Hreško J., Bugar G., 2015. *The recent timberline changes in the Tatra Mountains: A case study of the Mengusovská Valley (Slovakia) and the Rybi Potok Valley (Poland)*. Geographia Polonica, vol. 88, no. 2, pp. 71-84.

Kłapowa M., 1976. *Mapa zagrożenia lawinowego w Tatrach – Tatry Zachodnie. Wynik kartowania lawin śnieżnych zimą 1969/1970*. Map at a scale of 1:10,000, 8 sheets.

Kotarba A., 1992. *Natural environment and landscape dynamics of the Tatra Mountains*. Mountain Research and Development, vol. 12, no. 2, pp. 105-129.

Kotarba A., Starkel L., 1972. *Holocene morphogenetic altitudinal zones in the Carpathians*. Studia Geomorphologica Carpatho-Balcanica, 6, pp. 21-35.

Kozak J., 2005. *Zmiany powierzchni lasów w Karpatach Polskich na tle innych gór świata*. Kraków: Wydawnictwo Uniwersytetu Jagiellońskiego.

Körner C., 2003. *Limitation and stress – Always or never?* Journal of Vegetation Science, vol. 14, no. 2, pp. 141-143.

Körner C., 2004. *Individuals have limitations, not communities – A response to Marrs, Weiher and Lortie et al.* Journal of Vegetation Science, vol. 15, no. 4, pp. 581-582.

Körner C., 2012. *Alpine treelines: Functional ecology of the global high elevation tree limits*. Basel-London: Springer Science & Business Media.

Kulakowski D., Rixen C., Bebi P., 2006. *Changes in forest structure and in the relative importance of climatic stress as a result of suppression of avalanche disturbance*. Forest Ecology and Management, vol. 223, no. 1-3, pp. 66-74.

Kullman L., 2010. *One century of treeline change and stability – Experiences from the Swedish Scandes*. Landscape Online,17, pp. 1-31.

Lara A., Villalba R., Wolodarsky-Franke A., Aravena J.C., Luckman B.H., Cuq E., 2005. *Spatial and temporal variation in Nothofagus pumilio growth at tree line along its latitudinal range (35 40'–55 S) in the Chilean Andes*. Journal of Biogeography, vol. 32, no. 5, pp. 879-893.

Lempa M., Kaczka R.J., Rączkowska Z., Janecka K., 2016. *Combining tree-ring dating and geomorphological analyses in the reconstruction of spatial patterns of the runout zone of snow avalanches, the Rybi Potok Valley, the Tatra Mountains*. Geographia Polonica, vol. 89, no. 1, pp. 31-45.

Maggioni M., Gruber U., Stoffel A., 2002. *Definition and characterisation of potential avalanche release areas*. Proceedings of the ESRI Conference, San Diego.

Map of the Tatras, 1934. *Tatra Mountains (Polish part).* Photogrametric Map of the National Park (Tatra Mountains, Polish part), 1:20,000, Tourist-skiing edition.

Map of the Tatras, 1999/2000. *Tatra National Park – Winter*. 1:25,000, Warszawa: Polkart.

Marek R., 1910. *Waldgrenzstudien in den österreichischen Alpen*. Gotha: J. Perthes.

Micallef A., Berndt C., Masson D.G., Stow D.A., 2007. *A technique for the morphological characterization of submarine landscapes as exemplified by debris flows of the Storegga Slide*. Journal of Geophysical Research: Earth Surface, vol. 112, no. F02001.

Niculiță M., 2015. *Automatic extraction of landslides flow direction using geometric processing and DEMs* [in:] J. Jasiewicz, Z. Zwoliński, H. Mitasova, T. Hengl (eds.), Geomorphometry for Geosciences, Poznań: Bogucki Wydawnictwo Naukowe, pp. 201-204.

Paulsen J., Weber U.M., Körner C., 2000. *Tree growth near treeline: Abrupt or gradual reduction with altitude*. Arctic, Antarctic and Alpine Research, vol. 32, no. 1, pp. 14-20.

Pike R.J., 2000. *Geomorphometry-diversity in quantitative surface analysis*. Progress in Physical Geography, vol. 24, no. 1, pp. 1-20.

Plesník P., 1959. *Die obere Waldgrenze in den Westkarpaten*. Wissenschaftliche Zeitschrift der Martin-Luther-Universität, vol. 8, no. 2, Halle-Wittenberg: Martin-Luther-Universität.

Price L.W., 1981. *Mountain and man*. Berkeley-Los Angeles-Paris: University of California Press.

Rubner K., 1953. *Die pflanzengeographischen Grundlagen des Waldbaus*. Radebeul-Berlin: Neumann Verlag.

Sarmiento F.O., 2002. *Anthropogenic change in the landscapes of highland Ecuador*. Geographical Review, vol. 92, no. 2, pp. 213-234.

Schumm S.A., 1956. *Evolution of drainage systems and slopes in badlands at Perth Amboy, New Jersey*. Geological Society of America Bulletin, vol. 67, no. 5, pp. 597-646.

Shandra O., Weisberg P., Martazinova V., 2013. *Influences of climate and land use history on forest and timberline dynamics in the Carpathian Mountains during the twentieth century* [in:] J. Kozak, K. Ostapowicz, A. Bytnerowicz, B. Wyżga (eds.), The Carpathians: Integrating nature and society towards sustainability, Environmental Science and Engineering. Berlin-Heidelberg: Springer-Verlag, pp. 209-223.

Sokołowski M., 1928. *O górnej granicy lasu w Tatrach*. Kraków: Zakłady Kórnickie.

Stacey K., MacGregor M., 1999. *Learning the algebraic method of solving problems*. The Journal of Mathematical Behavior, vol. 18, no. 2, pp. 149-167.

Tachikawa T., Kaku M., Iwasaki A., Gesch D., Oimoen M., Zhang Z., Danielson J., Krieger T., Curtis B., Haase J., Abrams M., Crippen R., Carabajal C., 2011. *ASTER Global Digital Elevation Model Version 2 – Summary of validation results*. Technical report, Earth Resources Observation and Science (EROS) Center (Geography).

Tchoukanski I., 2012. EasyCalculate 10. Plug-in for ArcGIS software, www.ian-ko.com/free/EC10/EC10_main.htm [15 January 2016].

Treml V., Banaš M., 2000. *Alpine timberline in The High Sudeties*. Acta Universitatis Carolinae, Geographica, Praha, 35, pp. 83-99.

Treml V., 2007. *The effect of terrain morphology and geomorphic processes on the position and dynamics of the alpine timberline. A case study from the High Sudetes, Czech Republic* [in:] A.S. Goudie, J. Kalvoda (eds.), Geomorphological variations, Prague: P3K, pp. 298-312.

Tribe A., 1992. *Automated recognition of valley lines and drainage networks from grid digital elevation models: A review and a new method*. Journal of Hydrology, vol. 139, no. 1, pp. 263-293.

Troll C., 1972. *Geoecology and world-wide differentiation of high-mountain ecosystems* [in:] C. Troll (ed.), Geoecology of the High-Mountain Regions of Euroasia. Wiesbaden: Steiner, pp. 264-275.

Troll C., 1988. *Comparative geography of the high mountains of the world in the view of landscape ecology* [in:] N.J.R. Alan, G.W. Knap, C. Stadel (eds.), Human impact on mountains, Totowa: Rowman & Littlefield, pp. 36-56.

Van Bogaert R., Haneca K., Hoogesteger J., Jonasson C., De Dapper M., Callaghan T.V., 2011. *A century of tree line changes in sub-Arctic Sweden shows local and regional variability and only a minor influence of 20th century climate warming*. Journal of Biogeography, vol. 38, no. 5, p. 907-921.

Veblen T.T., Hadley K.S., Nel E.M., Kitzberger T., Reid M., Villalba R., 1994. *Disturbance regime and disturbance interactions in a Rocky Mountain subalpine forest*. Journal of Ecology, vol. 82, no. 1, pp. 125-135.

Walsh S.J., Butler D.R., Allen T.R., Malanson G.P., 1994. *Influence of snow patterns and snow avalanches on the alpine treeline ecotone*. Journal of Vegetation Science, vol. 5, no. 5, pp. 657-672.

Walsh S.J., Butler D.R., Malanson G.P., Crews-Meyer K.A., Messina J.P., Xiao N., 2003. *Mapping, modeling, and visualization of the influences of geomorphic processes on the alpine treeline ecotone, Glacier National Park, MT, USA*. Geomorphology, vol. 53, no. 1, pp. 129-145.

Walter H., 1968. *Die Vegetation der Erde in ökophysiologischer Betrachtung. Bd. II*. Die gemäßigten und arktischen Zonen, Stuttgart: Fischer.

Walter H., Medina E., 1969. *Die Bodentemperatur als ausschlaggebender Faktor für die Gliederung der subalpinen und alpinen Stufe in den Anden Venezuelas (Vorläufige Mitteilung)*. Berichte der Deutschen Botanischen Gesellschaft, vol. 82, no. 3-4, pp. 275-281.

Wright R.D., Mooney H.A., 1965. *Substrate-oriented distribution of bristlecone pine in the White Mountains of California*. The American Midland Naturalist Journal, vol. 73, no. 2, pp. 257-284.

Zhao F., Zhang B., Pang Y., Yao Y., 2014. *A study of the contribution of mass elevation effect to the altitudinal distribution of timberline in the Northern Hemisphere*. Journal of Geographical Sciences, vol. 24, no. 2, pp. 226-236.

Zientarski J., 1985. *Wpływ wzniesienia oraz wielkości masywu górskiego na kształtowanie się górnej granicy lasu w Polsce*. Poznań: Akademia Rolnicza [PhD thesis].

Żmudzka E., 2011. *Współczesne zmiany klimatu wysokogórskiej części Tatr*. Prace i Studia Geograficzne, 47, pp. 217-226.

Žiak M., 2012. *Lavínová hrozba, bilancia energie a hmoty vo vysokohorskom prostredí*. Bratislava: Prírodovedecká fakulta Univerzity Komenského v Bratislave [PhD thesis].

Žiak M., Długosz M., 2015. *Potencjalne obszary lawinowe*. Chart V.3 [in:] K. Dąbrowska, M. Guzik (eds.), Atlas Tatr. Przyroda nieożywiona. Zakopane: Tatrzański Park Narodowy.

Article first received • October 2015
Article accepted • February 2016